ORIGINAL ARTICLE

Effect of the specific proteasome inhibitor bortezomib on cancer-related muscle wasting

Fabio Penna[1†], Andrea Bonetto[2†], Zaira Aversa[3], Valerio Giacomo Minero[4,5], Filippo Rossi Fanelli[3], Paola Costelli[1] & Maurizio Muscaritoli[3]*

[1]Department of Clinical and Biological Sciences, University of Turin, Turin, Italy; [2]Department of Surgery, Indiana University School of Medicine, IUPUI, Indianapolis, IN, USA; [3]Department of Clinical Medicine, Sapienza, University of Rome, Rome, Italy; [4]Center of Experimental Research and Medical Studies (CeRMS), Città della Salute e della Scienza, Turin, Italy; [5]Department of Molecular Biotechnology and Health Sciences, University of Turin, Turin, Italy

Abstract

Background   Muscle wasting, a prominent feature of cancer cachexia, is mainly caused by sustained protein hypercatabolism. The enhanced muscle protein degradation rates rely on the activity of different proteolytic systems, although the Adenosine triphosphate (ATP)-ubiquitin-proteasome-dependent pathway and autophagy have been shown to play a pivotal role. Bortezomib is a potent reversible and selective proteasome and NF-κB inhibitor approved for the clinical use, which has been shown to be effective in preventing muscle wasting in different catabolic conditions. The aim of the present study has been to investigate whether pharmacological inhibition of proteasome by bortezomib may prevent skeletal muscle wasting in experimental cancer cachexia.

Methods   Cancer cachexia was induced in rats by intraperitoneal injection of Yoshida AH-130 ascites hepatoma cells and in mice by subcutaneous inoculation of C26 carcinoma cells. Animals were then further randomized to receive bortezomib. The AH-130 hosts were weighted and sacrificed under anaesthesia, on Days 3, 4, 5, and 7 after tumour inoculation, while C26-bearing mice were weighted and sacrificed under anaesthesia 12 days after tumour transplantation. NF-κB and proteasome activation, MuRF1 and atrogin-1 mRNA expression and beclin-1 protein levels were evaluated in the gastrocnemius of controls and AH-130 hosts.

Results   Bortezomib administration in the AH-130 hosts, although able to reduce proteasome and NF-κB DNA-binding activity in the skeletal muscle on Day 7 after tumour transplantation, did not prevent body weight loss and muscle wasting. In addition, bortezomib exerted a transient toxicity, as evidenced by the reduced food intake and by the increase in NF-κB DNA-binding activity in the AH-130 hosts 3 days after tumour transplantation. Beclin-1 protein levels were increased by bortezomib treatment in Day 3 controls but were unchanged on both Days 3 and 7 in the AH-130 hosts, suggesting that an early compensatory induction of autophagy may exist in healthy but not in tumour-bearing animals. Regarding C26-bearing mice, bortezomib did not prevent as well body and muscle weight loss 12 days after tumour implantation.

Conclusions   The results obtained suggest that proteasome inhibition by bortezomib is not able to prevent muscle wasting in experimental cancer cachexia. Further studies are needed to address the issue whether a different dosage of bortezomib alone or in combination with other drugs modulating different molecular pathways may effectively prevent muscle wasting during cancer cachexia.

Keywords   Cancer cachexia; Muscle wasting; Proteasome; Bortezomib

Introduction

Muscle wasting is by far the most clinically relevant feature of cancer cachexia, a life-threatening syndrome associated with poor prognosis and impaired quality of life.[1] The mechanisms underlying muscle wasting in cancer cachexia are not yet fully understood, but studies performed in experimental models as well as in neoplastic patients have shown that a prominent role is played by sustained protein hypercatabolism.[2] The enhanced muscle protein degradation rates result from hyperactivation of different proteolytic systems, but the degradative pathways dependent on proteasome and autophagy have been shown to play a prominent role.[3,4] The former relies on ubiquitylation of target proteins, which are subsequently degraded by the 26S proteasome, a multicatalytic complex, that contains a core (20S proteasome), which is characterized by five different peptidase activities: trypsin-like, chymotrypsin-like, peptidyl-glutamyl peptidase, branched-chain amino acid-preferring, and small-neutral amino acid-preferring activities.[5]

Several chemical compounds able to inhibit proteasome activity have been described including peptide analogues of substrates with different C-terminal groups such as aldehydes, epoxyketones, boronic acids, and vinyl sulfones.[6,7] Interestingly, different proteasome inhibitors have proved effective in preventing muscle wasting in many experimental conditions such as sepsis, burn injury, cancer, immobilization, and denervation atrophy.[8–12] However, in recent years, bortezomib has attracted particular attention, as it was the first proteasome inhibitor approved for clinical use.[13] Bortezomib is a selective dipeptide boronic acid analogue that works primarily by reversible inhibition of the chymotrypsin-like site in the β5-subunit of the 20S proteasome, but it can also inhibit the caspase-like site (β1-subunit) at high concentration and minimally affect the trypsin-like site (β2-subunit).[14–16] Proteasome blockade by bortezomib results in many effects such as inhibition of angiogenesis, of NF-κB activation, and of cytokine and growth factor production, apoptosis induction, cell cycle arrest.[17,18] Bortezomib has been approved by the Food and Drug Administration in 2003 as a third-line treatment for relapsed and refractory multiple myeloma,[19] in 2005 for multiple myeloma progressing after at least one prior therapy,[20] and in 2008, it has been evaluated in a phase III clinical trial also as front-line treatment for newly diagnosed multiple myeloma patients.[21,22] Bortezomib is also approved for mantle cell lymphoma,[23] and trials in other conditions are in progress.[24–28]

Bortezomib has been reported to effectively prevent muscle wasting in different experimental catabolic conditions associated with proteasome hyperactivation such as burn injury,[29] denervation atrophy,[30] diaphragm weakness in COPD,[31] and Duchenne muscular dystrophy.[32,33] However, bortezomib has been shown to only partially attenuate muscle atrophy caused by hindlimb casting[34] and to prevent endotoxin-induced diaphragm weight loss but not specific force reduction.[35] As for cancer cachexia, bortezomib has been recently reported to be unable to restore muscle mass in mice implanted with LP07 adenocarcinoma,[36,37] and a subanalysis from two clinical trials suggested that bortezomib does not attenuate weight loss in patients with advanced pancreatic cancer.[38] These observations, however, do not rule out that bortezomib may be effective in treating cancer-related muscle wasting as differences in the level of proteasome activity may exist among different tumour stages as well as in different tumour types.[39–42] Indeed, while proteasome activity is increased in the skeletal muscle of gastric cancer patients and correlates with disease severity,[39,40] it is not modified in the skeletal muscle of esophageal[41] and non-small cell lung cancer patients.[42] This would suggest that proteasome inhibition may differentially affect cancer-related muscle wasting; hence, the role of bortezomib in the treatment of cancer cachexia is still incompletely understood.

In the present study, we therefore investigated whether pharmacological inhibition of proteasome by bortezomib may attenuate skeletal muscle wasting in rats bearing the Yoshida AH-130 ascites hepatoma, a well-described model of cancer cachexia associated to hyperactivation of the ubiquitin-proteasome pathway.[43–46] Additional experiments were performed to evaluate bortezomib effectiveness in preventing body and muscle weight loss in mice implanted with the C26 colon adenocarcinoma, another experimental model of cancer cachexia associated to severe muscle wasting.[47,48]

Material and methods

Animals

Experimental animals were cared for in compliance with the Italian Ministry of Health Guidelines (no. 86609 EEC, permit number 106/2007-B) and the Policy on Humane Care and Use of Laboratory Animals (NIH 1996). The experimental protocol was approved by the Bioethical Committee of the University of Turin (Turin, Italy).

Male Wistar rats weighing approximately 150 g and male Balb-c mice weighing approximately 20 g were obtained from Charles River Laboratories (Calco, Italy) and were maintained on a regular dark-light cycle (light from 8 a.m. to 8 p.m.), with free access to food and water during the whole experimental period.

Tumour-bearing rats received an i.p. inoculum of approximately 10^8 Yoshida AH-130 ascites-hepatoma cells whereas tumour-bearing mice were inoculated s.c. dorsally with 5×10^5 C26 carcinoma cells. Control rats and mice were inoculated with a correspondent volume of vehicle (saline). Animals (rats or mice) were then further randomized to receive bortezomib (Velcade®, Millennium Pharmaceuticals, Cambridge MA, USA) or corresponding volume of vehicle

(saline). In particular, two days after transplantation, rats were administered bortezomib (0.25 mg/kg, i.v., single dose), while mice received the drug (0.5 mg/kg, i.v.) on Day 7 after tumour transplantation and 4 h before sacrifice. The dose was chosen in view of results obtained in dose-response experiments (data not shown).

Animal weight and food intake were recorded daily throughout the entire experiment.

As for the AH-130 hosts, on Days 3, 4, 5, and 7 after tumour inoculation, rats were weighted and sacrificed under anaesthesia; mice were sacrificed under anaesthesia 12 days after C26 transplantation. Muscles and organs were rapidly excised, weighed, frozen in liquid nitrogen, and stored at −80°C until analysis.

Western blot

Approximately 50 mg of gastrocnemius muscle was homogenized in 80 mmol/L Tris-HCl, pH 6.8, containing 100 mmol/L dithiothreitol, 70 mmol/L Sodium dodecyl sulfate (SDS), and 1 mmol/L glycerol, with freshly added protease and phosphatase inhibitor cocktails; kept on ice for 30 min; centrifuged at 15 000 g for 10 min at 4°C and the supernatant collected. Protein concentration was assayed according to Bradford using bovine serum albumin as working standard. Equal amounts of protein (30 mg) were heat denatured in sample-loading buffer (50 mmol/L Tris-HCl, pH 6.8, 100 mmol/L dithiothreitol, 2% SDS, 0.1% bromophenol blue, 10% glycerol), resolved by SDS-PolyAcrylamide Gel Electrophoresis (PAGE), and transferred to nitrocellulose membranes (Bio- Rad Laboratories, Hercules, CA). The filters were blocked with Tris-buffered saline containing 0.05% Tween and 5% non-fat dry milk and incubated overnight with an antibody directed against beclin-1 (B6186, Sigma, St. Louis, MO, USA). A mouse monoclonal anti-rat α-tubulin antibody (T5168, Sigma-Aldrich, St. Louis, MO) was used for loading control. Peroxidase-conjugated IgG (Bio-Rad Laboratories) were used as secondary antibodies. Immunoreactive protein bands were detected by enhanced chemoluminescence. Quantification of the bands was performed by densitometric analysis using specific software version 2006c (TotalLab; Nonlinear Dynamics, Newcastle on Tyne, UK).

Proteasome activity

Proteasome chymotrypsin-like activity in the gastrocnemius was determined by cleavage of a specific fluorogenic substrate as previously described.[43,40]

Briefly, gastrocnemius was homogenized in 20 mM Tris–HCl, pH 7.2, containing 0.1 mM EDTA, 1 mM 2-mercaptoethanol, 5 mM ATP, 20% glycerol, 0.04% (v/v) Nonidet P-40. Muscle homogenates were then centrifuged at 13 000 g for 15 min at 4°C. The supernatant was collected and protein concentration determined as described in the previous text. Aliquots of 50 µg

protein were then incubated for 60 min at 37°C in the presence of the fluorogenic substrate succinyl-Leu-Leu-Val-Tyr-7-amino-methyl-coumarin (LLVY, Sigma, St. Louis, MO, USA). The incubation buffer was 50 mM Hepes, pH 8.0, containing 5 mM Ethylene glycol-bis(2-aminoethylether)-N,N,N',N'-tetraacetic acid (EGTA). Fluorescence was read with a spectrofluorometer (excitation: 380 nm, emission: 460 nm; Perkin–Elmer,Norwalk, CT, USA). The activity, expressed as nkatal/mg protein, was calculated by using free amino-methyl-coumarin as working standard.

Electrophoretic mobility shift assay

To prepare nuclear extracts, gastrocnemius (100 mg) was homogenized in ice-cold 10 mm 4-(2-Hydroxyethyl)piperazine-1-ethanesulfonic acid (HEPES), pH 7.5, containing 10 mM MgCl$_2$, 5 mM KCl, 0.1 mM EDTA pH 8.0, 0.1% Triton X-100, 0.1 mM phenylmethanesulfonyl fluoride, 1 mM DL-Dithiothreitol (DTT), 2 µg/ml aprotinin, 2 µg/ml leupeptin. Samples were centrifuged (5 min, 3000 g), pellets resuspended in ice-cold 20 mM HEPES, pH 7.9, containing 25% glycerol, 500 mM NaCl, 1.5 mM MgCl$_2$, 0.2 mM EDTA, pH 8.0, 0.2 mM phenylmethanesulfonyl fluoride, 0.5 mM DTT, 2 µg/ml aprotinin, 2 µg/ml leupeptin, and incubated on ice for 30 min. Cell debris were removed by centrifugation (5 min, 3000 g), the supernatant collected and stored at −80°C. NF-κB oligonucleotides were purchased from Promega Italia (Milano, Italy). Oligonucleotide labelling and binding reactions were performed by using the Gel Shift Assay System (Promega, Milan, Italy). Binding reaction mixtures, containing nuclear proteins (10 µg) and gel shift binding buffer [10 mm Tris-HCl, pH 7.5, containing 1 mM MgCl$_2$, 0.5 mM EDTA, 0.5 mM DTT, 50 mM NaCl, 0.05 µg//µL poly(dI-dC)·poly(dI-dC), 4% glycerol], were incubated (10 min) at room temperature in the presence of 0.035 pmol ^{32}P-ATP end-labelled double-stranded oligonucleotide. After incubation, samples were electrophoresed in 0.5× Tris-Borate-EDTA buffer at 350 V for 40 min on a 4% non-denaturing acrylamide gel. The gel was dried (45 min) and exposed overnight or longer to an autoradiography film (GE Healthcare, Milan, Italy) at −80°C with intensifying screens. Bands specificity was confirmed by adding an excess amount of a specific oligonucleotide (1.75 pmol) to a control gastrocnemius sample. HeLa cell nuclear extract was used as positive control (Promega, Milan, Italy).

Semi-quantitative reverse transcriptase (RT)-PCR

Total RNA was extracted from the gastrocnemius muscle with the TriPure reagent (Roche, Indianapolis, USA), and quantified spectrophotometrically. RNA integrity was checked by electrophoresis on 1.2% agarose gel, containing 10% 3-(N-morpholino) propanesulfonic acid (MOPS) 0.2 M and 18% formaldehyde.

Atrogin-1 and MuRF1 mRNA levels were analysed by semi-quantitative reverse-transcription polymerase chain reaction

using the kit 'Ready-to-Go RT-PCR Beads' (Hybond C, Amersham Italia, Milano, Italy). Aliquots of total RNA (0.5 μg) were added to a RT-PCR reaction mixture containing PCR buffer (10 mM Tris-HCl pH 9.0, 60 mM KCl, 1.5 mM $MgCl_2$), Taq DNA-polymerase 2.0 units, 10 μM of each primer, and 200 μM deoxynucleotide triphosphate (dNTP). Primers for atrogin-1, MuRF1, and Glyceraldehyde 3-phosphate dehydrogenase (GAPDH), described in *Table* 1, were obtained according to published sequences (Invitrogen, Milano, Italy).

Amplification conditions consisted of 1 min denaturation at 95°C, 1 min annealing at 60°C, and 2 min polymerization at 72°C for each step for 25 cycles and extension at 72°C for 7 min. Positive and negative controls have been performed. PCR products were electrophoresed on 2% agarose gels and visualized with ethidium bromide. A standard DNA ladder was used to estimate the length of each PCR product. Quantification was performed by densitometric analysis: individual product bands and representative background were excised from each gel lane and analysed by means of a specific software (Phoretix). The results were normalized according to 18S ribosomal subunit expression, amplified with the following conditions: denaturation (95°C, 30 s), annealing (55°C, 1 min), polymerization (72°C, 2 min), for 10 cycles, and extension (72°C, 7 min). Comparisons among groups have been made in the linear phase of amplification.

Statistical analysis

Results are reported as means ± SD. Statistical analysis was performed by using the Student's *t*-test or one-way analysis of variance followed by Tukey's post-hoc test as appropriate. $P < 0.05$ was considered statistically significant.

Results

The growth of the Yoshida AH-130 hepatoma determined in the hosts a progressive body and gastrocnemius weight loss (*Figure* 1A and B), consistent with previous studies using the same experimental model.[45,49] Treatment with bortezomib did not affect cancer-induced body and muscle weight loss on Day 3 after tumour inoculum, while on Day 7, it worsened the cachectic phenotype (*Figure* 1A and B). As for the liver (*Figure* 2A), it was reduced in size in tumour hosts starting from Day 5 after transplantation. Bortezomib treatment lead to an increase of liver mass in Day 4 controls

Figure 1 Bortezomib does not prevent body and gastrocnemius muscle weight loss in AH-130-bearing rats. (A) Body and (B) gastrocnemius weight were evaluated in controls (C) and tumour-bearing rats (AH-130) treated or untreated with bortezomib (BTZ) at Day 3 (d3) and Day 7 (d7) after AH-130 cell inoculation. Results (means ± SD) are expressed as percentage of controls (C and C + BTZ: *n* = 4; AH-130, AH-130 + BTZ: *n* = 8). *$P < 0.05$, **$P < 0.01$, ***$P < 0.001$ vs. control.
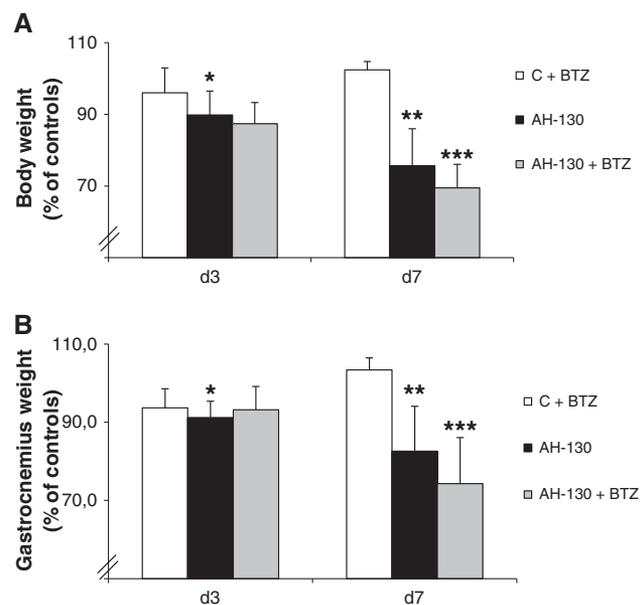
only. No effect of bortezomib administration could be observed in controls at Days 3, 5, and 7 or in the tumour hosts (Days 3–7). No significant differences in spleen weight were observed in control and tumour-bearing rats treated with bortezomib (*Figure* 2B). Food consumption in control rats was not modified by bortezomib (*Figure* 3A). In contrast, the drug exerted a marked reduction of food intake on Day 3 in tumour-bearing rats (24 h after the first administration), when tumour-induced anorexia is not yet detectable in this experimental model. Such a reduction was likely due to a transient toxic effect of the drug. Indeed, at the subsequent time points (Days 5 and 7), the reduced food intake that characterizes tumour-bearing rats was not further affected by bortezomib treatment (*Figure* 3A). No significant changes were observed for water intake among all the experimental groups (*Figure* 3B).

Tumour growth, evaluated as total cell number, was reduced by bortezomib treatment on Days 4 and 5 after implantation, but on Day 7, it was comparable in treated and untreated tumour-bearing rats (*Figure* 4), suggesting the development of chemoresistance.

Table 1 Oligonucleotide sequences

Gene	Primer sequence	NCBI reference sequence
Atrogin-1	5'-CCATCAGGAGAAGTGGATCTATGTT-3' 3'-GCTTCCCCCAAAGTGCAGTA-5'	AY059628.1
MuRF-1	5'-GGACGGAAATGCTATGGAGA-3' 3'-AACGACCTCCAGACATGGAC-5'	AY059627.1
GAPDH	5'-GGTGAAGGTCGGAGTCAACG-3' 3'-CAAAGTTGTCATGGATGACC-5'	M17701.1

NCBI, National Center for Biotechnology Information

Figure 2 Effects of bortezomib on liver and spleen weight. (A) Liver and (B) spleen weight were evaluated in controls (C) and tumour-bearing rats (AH-130) treated or untreated with bortezomib (BTZ) at Day 3 (d3), Day 4 (d4), Day 5 (d5), and Day 7 (d7) after AH-130 cell inoculation. Results (means ± SD) are expressed as percentage of controls (C and C + BTZ: $n = 4$; AH-130, AH-130 + BTZ: $n = 8$). *$P < 0.05$, **$P < 0.01$ vs. control; ¶$P < 0.05$ vs. C + BTZ.
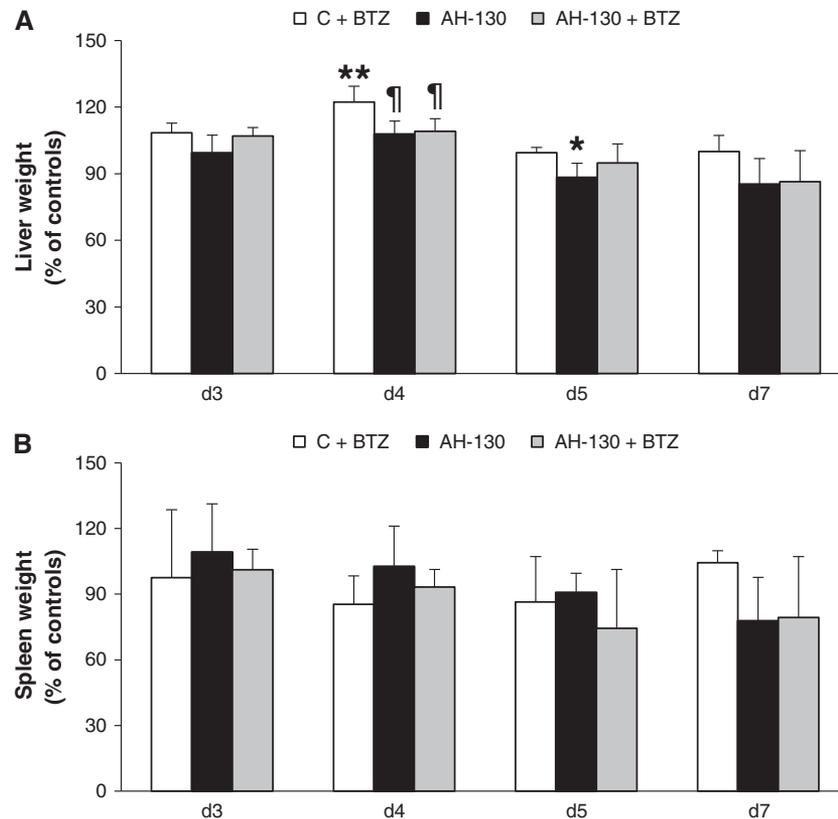
Bortezomib inhibitory activity is mainly exerted by blocking proteasome chymotrypsin-like sites.[17] In this regard, previous studies showed that chymotrypsin-like activity is increased in the gastrocnemius of rats bearing the AH-130 hepatoma.[44,46] In the present study, chymotrypsin-like activity in the gastrocnemius of treated rats was significantly reduced compared with those of untreated animals (treated controls: 25% residual activity vs. untreated rats, $P < 0.0001$; treated AH-130: 70% residual activity vs. untreated tumour hosts, $P < 0.05$), demonstrating that the bortezomib dosage adopted was indeed effective.

Data previously reported in the literature show that the inhibition of proteasome activity prevents IκB degradation and subsequent activation and nuclear translocation of NF-κB.[7] Consistently, the results shown in *Figure* 5 demonstrate that bortezomib treatment at Day 7 after tumour implantation significantly reduced NF-κB DNA-binding activity in the gastrocnemius of AH-130 hosts (*Figure* 5). Surprisingly enough, a significant increase in NF-κB DNA-binding activity was observed on Day 3 in tumour-bearing rats treated with bortezomib (*Figure* 5).

At any observation time, mRNA levels for atrogin-1 and MuRF1 were not affected by bortezomib administration (*Figure* 6).

Because bortezomib has been proposed to stimulate autophagy,[50–53] although not consistently,[54,55] the levels of beclin-1, an accepted marker of autophagic sequestration[56] were evaluated. Bortezomib treatment induced a significant increase of beclin-1 levels in control animals (Day 3). In contrast, beclin-1 expression was slightly, although not significantly, increased in tumour hosts and was not modified by bortezomib (*Figure* 7).

Finally, in order to assess if results obtained with bortezomib treatment were model-dependent, the experiment was repeated on mice bearing the colon 26 (C26). Consistently with previous experiments,[57] the growth of the C26 tumour induced in the host mice a significant reduction of food intake, body weight, and gastrocnemius weight; all these parameters were not affected by bortezomib treatment 12 days after tumour implantation (*Figure* 8). Spleen and tumour weight were also not significantly modified by bortezomib treatment in the C26 hosts, while liver mass was significantly reduced (see Supporting Information).

Discussion

The results obtained in the present study show that bortezomib administration *in vivo*, although able to reduce

Figure 3 Effects of bortezomib on food and water intake. (A) Food intake and (B) water intake were evaluated daily in control (C) and tumour-bearing rats (AH-130) treated or untreated with bortezomib (BTZ). C and C + BTZ: *n* = 4; AH-130, AH-130 + BTZ: *n* = 8.
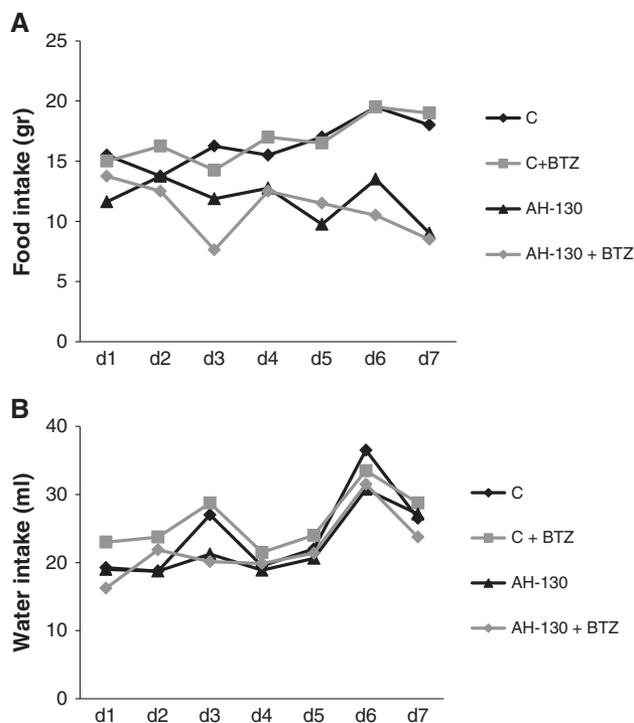

Figure 5 Bortezomib modulates NF-κB nuclear translocation in the gastrocnemius of the AH-130 hosts. (A) Densitometric analysis and (B) representative pattern of NF-κB DNA-binding activity measured by electrophoretic mobility shift assay in the gastrocnemius of control (C) and tumour-bearing rats (AH-130) treated or untread with bortezomib (BTZ) at Day 3 (d3) and Day 7(d7) after AH-130 cell inoculation. Results (means ± SD) are expressed as percentage of controls (C and C + BTZ: *n* = 4; AH-130, AH-130 + BTZ: *n* = 8). *$P < 0.05$ vs. control, §$P < 0.05$, §§$P < 0.01$ vs. AH-130.
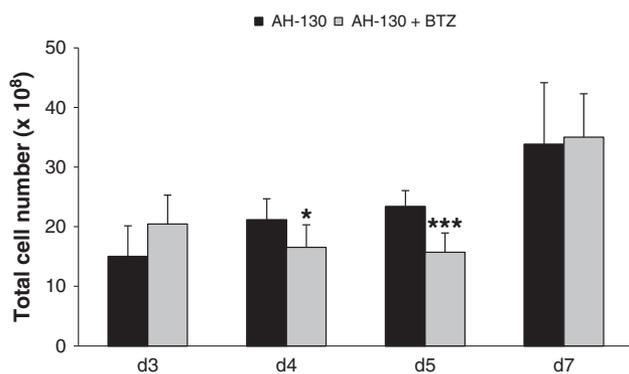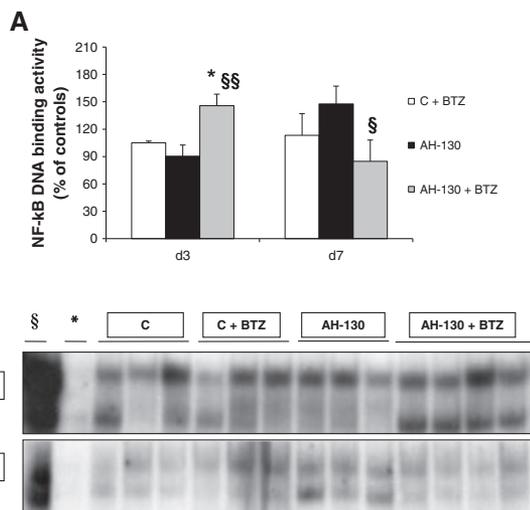

Figure 4 Effects of bortezomib on AH-130 cell number. Total cell number were evaluated in tumour-bearing rats (AH-130) treated or untreated with bortezomib (BTZ) at Day 3 (d3), Day 4 (d4), Day 5 (d5), and Day 7 (d7) after AH-130 cell inoculation. Results are expressed as means ± SD (C and C + BTZ: *n* = 4; AH-130, AH-130 + BTZ: *n* = 8). *$P < 0.05$, ***$P < 0.001$ vs. AH-130.

proteasome and NF-κB activity in the skeletal muscle, does not prevent body weight loss and muscle wasting in experimental cancer cachexia. These findings are in agreement with results obtained in LP07-bearing mice, where treatment with bortezomib failed in preventing cancer-related body and muscle weight loss.[36,37] These observations would suggest

that inhibition of a single proteolytic system is not effective in counteracting muscle wasting in cancer cachexia. Indeed, enhanced muscle protein breakdown in cancer cachexia has been demonstrated to depend on the activity of different degradative mechanisms besides proteasome, such as the autophagic-lysosomal pathway and the calcium-dependent proteases (calpains).[58,59]

Moreover, inhibition of a degradative pathway can have a negative impact on protein quality control and muscle performance. Indeed, the use of protein degradation inhibitors could have major drawbacks such as promoting the accumulation of misfolded or aggregate-prone proteins.[60] This could be very toxic for the cell, in particular, if other degradative systems, such as autophagy, are not contemporarily and efficiently working to remove accumulated proteins. In the present study, beclin-1 protein levels were increased by bortezomib treatment in Day 3 controls but were unchanged on both Days 3 and 7 in the AH-130 hosts, suggesting that an early compensatory induction of autophagy exists in healthy but not in tumour-bearing animals. In this regard, recent observations have shown that the levels of p62, a marker of autophagosome disposal, markedly increase in the gastrocnemius of rats bearing the AH-130 hepatoma 7 days after tumour inoculum, in face of unchanged beclin-1 expression.[59] This observation suggests that a progressive exhaustion of the lysosomal degradative capacity occurs in the skeletal muscle of tumour-bearing animals. Therefore, upon proteasome inhibition, ubiquitylated protein

Figure 6 Bortezomib does not modulate atrogin-1 and MuRF1 mRNA levels in the gastrocnemius of the AH-130 hosts. mRNA levels for (A) atrogin-1 and (B) MuRF1 were determined by semi-quantitative RT-PCR in the gastrocnemius of controls (C) and tumour-bearing rats (AH-130) treated or untread with bortezomib (BTZ) at Day 3 (d3) and Day 7 (d7) after AH-130 cell inoculation. Results (means ± SD) are expressed as percentage of controls (C and C + BTZ: $n = 4$; AH-130, AH-130 + BTZ: $n = 8$). **$P < 0.01$, ***$P < 0.001$ vs. control.
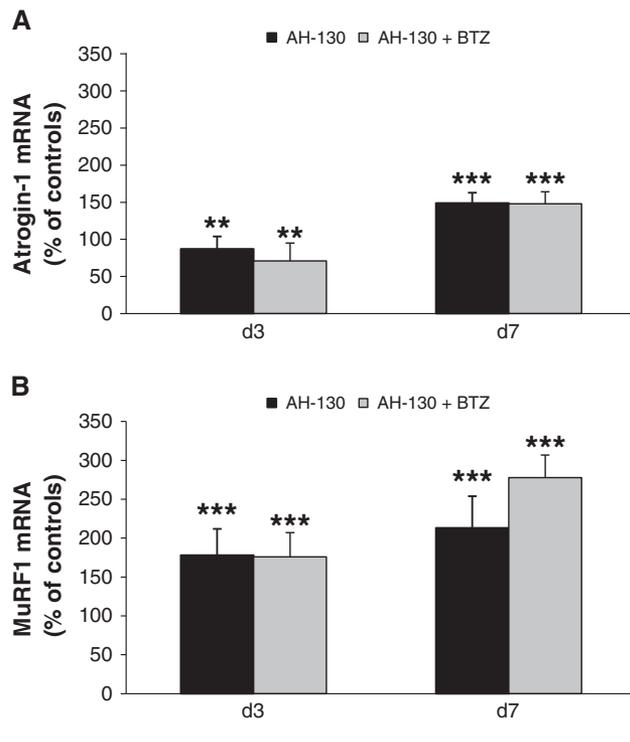

Figure 7 Bortezomib does not modulate beclin-1 protein levels in the gastrocnemius of the AH-130 hosts. Beclin-1 protein levels in gastrocnemius muscle of controls (C) and tumour-bearing rats (AH-130) treated and untreated with bortezomib (BTZ) at Day 3 (d3) and Day 7 (d7) after AH-130 cell inoculation were evaluated by western blotting. α-tubulin was used as loading control. Densitometric quantification are shown in the figure, and results (means ± SD) are expressed as percentage of controls (C and C + BTZ: $n = 4$; AH-130, AH-130 + BTZ: $n = 8$). *$P < 0.05$ vs. control.
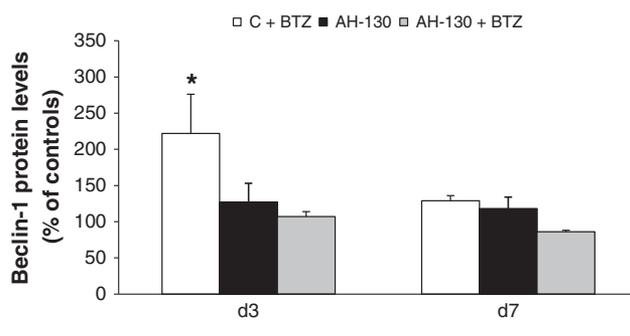
aggregates might not be efficiently removed because of impaired autophagic degradation, which could partially explain the worsened cachectic phenotype observed in the gastrocnemius of bortezomib-treated AH-130 hosts. All this reasoning, however, remains speculative because the amount of ubiquitylated protein was not assessed. Further experiments would be needed to clarify this point.

Besides autophagy, other mechanisms participate to the disposal of ubiquitin conjugates, such as deubiquitylating enzymes.[17,61] Little is known about deubiquitylation and its role in cancer-induced muscle wasting; however, an alteration of this process may play a role in the lack of effect of bortezomib administration to tumour-bearing animals.

In contrast with the results shown in the present study, treatment with a different proteasome inhibitor, namely MG132, has been reported to attenuate body weight loss and muscle depletion in mice bearing the C26 colon adenocarcinoma.[62] Such a discrepancy could rely on the fact that MG132 does not just inhibit proteasome, but also cathepsins and calpains.[6] In addition, MG132 administration, unlike bortezomib in our experiment, caused a significant reduction of C26 mass,[62] which could have contributed to improve skeletal muscle wasting.

Finally, additional specific effects of bortezomib besides proteasome inhibition may have affected the modulation of muscle mass in the present study. In this regard, bortezomib has been recently reported to inhibit differentiation, to arrest cell growth at G2/M phase, and to induce apoptosis in C2C12 myocyte cultures.[63] Importantly, although bortezomib is less toxic compared with other proteasome inhibitors, several side effects have been reported such as asthenia (due to fatigue and weakness), gastrointestinal events (i.e. nausea, diarrhoea, vomiting, and poor appetite), haematological toxicity (low platelets and erithrocytes count),[13] peripheral neuropathy,[64] and cardiotoxicity.[65–67] In the present experiment, bortezomib exerted a transient toxicity in tumour-bearing rats as evidenced by reduced food intake and increased NF-κB DNA-binding activity at Day 3 after tumour transplantation, which could have contributed, at least in part, to the lack of effectiveness in preventing cancer-related muscle wasting.

On the whole, the results shown in the present study demonstrate that proteasome inhibition by bortezomib is not able to prevent muscle wasting in tumour-bearing animals. However, the molecular mechanisms occurring in the skeletal muscle in response to bortezomib administration during cancer cachexia still need to be defined, and further studies should address the issue whether a different dosage of bortezomib alone or in combination with other drugs modulating different molecular pathways may effectively prevent muscle wasting during cancer cachexia.

Aknowledgements

Figure 8 Bortezomib does not affect food intake and does not prevent body and gastrocnemius muscle weight loss in C26-bearing mice. (A) Daily food intake, (B) body weight, and (C) gastrocnemius weight were evaluated in control (C) and tumour-bearing mice (C26) treated or untreated with bortezomib (BTZ) 12 days after C26 cell inoculation. Results (means ± SD) are expressed as percentage of controls (controls: *n* = 7; C26: *n* = 8; C26 + BTZ: *n* = 7). **$P < 0.001$ vs. control.
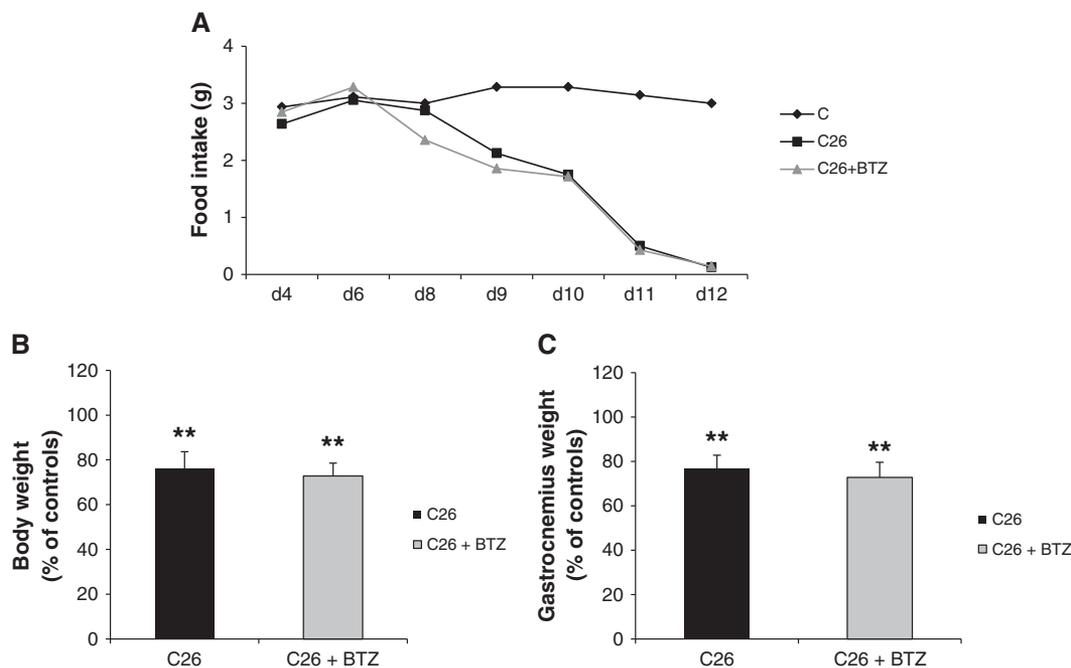
The authors certify that they comply with the ethical guidelines for authorship and publishing of the Journal of Cachexia, Sarcopenia and Muscle (von Haehling S, Morley JE, Coats AJS, Anker SD. Ethical guidelines for authorship and publishing in the Journal of Cachexia, Sarcopenia and Muscle. J Cachexia Sarcopenia Muscle. 2010;1:7–8).

Supporting information

Supporting information is available at Journal of Cachexia, Sarcopenia and Muscle online.

Supplementary figure. Bortezomib does not affect liver, spleen, and tumour weight in C26-bearing mice (A) Liser, (B) spleen, and (C) tumour weight were evaluated in tumour-bearing mice (C26) treated or untreated with bortezomib (BTZ) 12 days after C26 cell inoculation. Results (means ± SD) are expressed as percentage of controls (controls: n = 7; C26: n = 8; C26 + BTZ: n = 7). **$P < 0.01$ vs. control.

Conflict of interest

None declared.

References

1. Muscaritoli M, Molfino A, Gioia G, Laviano A, Rossi Fanelli F. The "parallel pathway": a novel nutritional and metabolic approach to cancer patients. *Intern Emerg Med* 2011;**6**:105–12.
2. Muscaritoli M, Bossola M, Aversa Z, Bellantone R, Rossi Fanelli F. Prevention and treatment of cancer cachexia: new insight into an old problem. *Eur J Cancer* 2006;**42**:31–41.
3. Acharyya S, Guttridge DC. Cancer cachexia signaling pathways continue to emerge yet much still points to the proteasome. *Clin Cancer Res* 2007;**13**:1356–61.
4. Penna F, Baccino FM, Costelli P. Coming back: autophagy in cachexia. *Curr Opin Clin Nutr Metab Care* 2014;**17**:241–6.
5. Ciechanover A. The ubiquitin-proteasome proteolytic pathway. *Cell* 1994;**79**:13–21.
6. Kisselev AF, Goldberg AL. Proteasome inhibitors: from research tools to drug candidates. *Chem Biol* 2001;**8**:739–58.
7. Crawford LJ, Walker B, Irvine AE. Proteasome inhibitors in cancer therapy. *J Cell Commun Signal* 2011;**5**:101–10.
8. Fischer D, Gang G, Pritts T, Hasselgren PO. Sepsis-induced muscle proteolysis is prevented by a proteasome inhibitor *in vivo*. *Biochem Biophys Res Commun* 2000;**270**:215–21.
9. Fang CH, Wang JJ, Hobler S, Li BG, Fischer JE, Hasselgren PO. Proteasome blockers inhibit protein breakdown in skeletal muscle after burn injury in rats. *Clin Sci (Lond)* 1998;**95**:225–33.
10. Zhang L, Tang H, Kou Y, Li R, Zheng Y, Wang Q, *et al*. MG132-mediated inhibition of the ubiquitin-proteasome pathway ameliorates cancer cachexia. *J Cancer Res Clin Oncol* 2013a;**139**:1105–15.
11. Caron AZ, Haroun S, Leblanc E, Trensz F, Guindi C, Amrani A, *et al*. The proteasome inhibitor MG132 reduces immobilization-induced skeletal muscle atrophy in mice. *BMC Musculoskelet Disord* 2011;**12**:185.

12. Tawa NE Jr, Odessey R, Goldberg AL. Inhibitors of the proteasome reduce the accelerated proteolysis in atrophying rat skeletal muscles. *J Clin Invest* 1997;**100**:197–203.

13. Chen D, Frezza M, Schmitt S, Kanwar J, Dou QP. Bortezomib as the first proteasome inhibitor anticancer drug: current status and future perspectives. *Curr Cancer Drug Targets* 2011;**11**:239–53.

14. Elliott PJ, Ross JS. The proteasome: a new target for novel drug therapies. *Am J Clin Pathol* 2001;**116**:637–46.

15. Schwartz R, Davidson T. Pharmacology, pharmacokinetics, and practical applications of bortezomib. *Oncology (Williston Park)* 2004;**18**:14–21.

16. Dick LR, Fleming PE. Building on bortezomib: second-generation proteasome inhibitors as anti-cancer therapy. *Drug Discov Today* 2010;**15**:243–9.

17. Goldberg AL. Development of proteasome inhibitors as research tools and cancer drugs. *Cell Biol* 2012;**199**:583–8.

18. Kubiczkova L, Pour L, Sedlarikova L, Hajek R, Sevcikova S. Proteasome inhibitors - molecular basis and current perspectives in multiple myeloma. *J Cell Mol Med* 2014;**18**:947–61.

19. Richardson PG, Barlogie B, Berenson J, Singhal S, Jagannath S, Irwin D, *et al*. A phase 2 study of bortezomib in relapsed, refractory myeloma. *N Engl J Med* 2003;**348**:2609–17.

20. Kane RC, Farrell AT, Sridhara R, Pazdur R. United States Food and Drug Administration approval summary: bortezomib for the treatment of progressive multiple myeloma after one prior therapy. *Clin Cancer Res* 2006;**12**:2955–60.

21. San Miguel JF, Schlag R, Khuageva NK, Dimopoulos MA, Shpilberg O, Kropff M, *et al*. Bortezomib plus melphalan and prednisone for initial treatment of multiple myeloma. *N Engl J Med* 2008;**359**:906–17.

22. Mateos MV, Richardson PG, Schlag R, Khuageva NK, Dimopoulos MA, Shpilberg O, *et al*. Bortezomib plus melphalan and prednisone compared with melphalan and prednisone in previously untreated multiple myeloma: updated follow-up and impact of subsequent therapy in the phase III VISTA trial. *J Clin Oncol* 2010;**28**:2259–66.

23. Kane RC, Dagher R, Farrell A, Ko CW, Sridhara R, Justice R, *et al*. Bortezomib for the treatment of mantle cell lymphoma. *Clin Cancer Res* 2007;**13**:5291–4.

24. Buac D, Shen M, Schmitt S, Kona FR, Deshmukh R, Zhang Z, *et al*. From bortezomib to other inhibitors of the proteasome and beyond. *Curr Pharm Des* 2013;**19**:4025–38.

25. Bose P, Batalo MS, Holkova B, Grant S. Bortezomib for the treatment of non-Hodgkin's lymphoma. *Expert Opin Pharmacother* 2014;**15**:2443–59.

26. Herrera AF, Kim HT, Bindra B, Jones KT, Alyea EP 3rd, Armand P, *et al*. A phase II study of bortezomib plus prednisone for initial therapy of chronic graft-versus-host disease. *Biol Blood Marrow Transplant* 2014;**20**:1737–43.

27. Pai CC, Chen M, Mirsoian A, Grossenbacher SK, Tellez J, Ames E, *et al*. Treatment of chronic graft-versus-host disease with bortezomib. *Blood* 2014;**124**:1677–88.

28. Skrott Z, Cvek B. Linking the activity of bortezomib in multiple myeloma and auto-immune diseases. *Crit Rev Oncol Hematol* 2014;**92**:61–70.

29. Lang CH, Huber D, Frost RA. Burn-induced increase in atrogin-1 and MuRF-1 in skeletal muscle is glucocorticoid independent but downregulated by IGF-I. *Am J Physiol Regul Integr Comp Physiol* 2007;**292**:R328–36.

30. Beehler BC, Sleph PG, Benmassaoud L, Grover GJ. Reduction of skeletal muscle atrophy by a proteasome inhibitor in a rat model of denervation. *Exp Biol Med (Maywood)* 2006;**231**:335–41.

31. van Hees H, Ottenheijm C, Ennen L, Linkels M, Dekhuijzen R, Heunks L. Proteasome inhibition improves diaphragm function in an animal model for COPD. *Am J Physiol Lung Cell Mol Physiol* 2011;**301**:L110–6.

32. Bonuccelli G, Sotgia F, Capozza F, Gazzerro E, Minetti C, Lisanti MP. Localized treatment with a novel FDA-approved proteasome inhibitor blocks the degradation of dystrophin and dystrophin-associated proteins in mdx mice. *Cell Cycle* 2007;**6**:1242–8.

33. Gazzerro E, Assereto S, Bonetto A, Sotgia F, Scarfi S, Pistorio A, *et al*. Therapeutic potential of proteasome inhibition in Duchenne and Becker muscular dystrophies. *Am J Pathol* 2010;**176**:1863–77.

34. Krawiec BJ, Frost RA, Vary TC, Jefferson LS, Lang CH. Hindlimb casting decreases muscle mass in part by proteasome-dependent proteolysis but independent of protein synthesis. *Am J Physiol Endocrinol Metab* 2005;**289**:E969–80.

35. Supinski GS, Vanags J, Callahan LA. Effect of proteasome inhibitors on endotoxin-induced diaphragm dysfunction. *Am J Physiol Lung Cell Mol Physiol* 2009;**296**:L994–L1001.

36. Chacon-Cabrera A, Fermoselle C, Urtreger AJ, Mateu-Jimenez M, Diament MJ, de Kier Joffé ED, *et al*. Pharmacological strategies in lung cancer-induced cachexia: effects on muscle proteolysis, autophagy, structure, and weakness. *J Cell Physiol* 2014;**229**:1660–72.

37. Fermoselle C, García-Arumí E, Puig-Vilanova E, Andreu AL, Urtreger AJ, de KierJoffé ED, *et al*. Mitochondrial dysfunction and therapeutic approaches in respiratory and limb muscles of cancer cachectic mice. *Exp Physiol* 2013;**98**:1349–65.

38. Jatoi A, Alberts SR, Foster N, Morton R, Burch P, Block M, *et al*. Is bortezomib, a proteasome inhibitor, effective in treating cancer-associated weight loss? Preliminary results from the North Central Cancer Treatment Group. *Support Care Cancer* 2005;**13**:381–6.

39. Bossola M, Muscaritoli M, Costelli P, Bellantone R, Pacelli F, Busquets S, *et al*. Increased muscle ubiquitin mRNA levels in gastric cancer patients. *Am J Physiol Regul Integr Comp Physiol* 2001;**280**:R1518–23.

40. Bossola M, Muscaritoli M, Costelli P, Grieco G, Bonelli G, Pacelli F, *et al*. Increased muscle proteasome activity correlates with disease severity in gastric cancer patients. *Ann Surg* 2003;**237**:384–9.

41. Tardif N, Klaude M, Lundell L, Thorell A, Rooyackers O. Autophagic-lysosomal pathway is the main proteolytic system modified in the skeletal muscle of esophageal cancer patients. *Am J Clin Nutr* 2013;**98**:1485–92.

42. Op den Kamp CM, Langen RC, Minnaard R, Kelders MC, Snepvangers FJ, Hesselink MK, *et al*. Pre-cachexia in patients with stages I-III non-small cell lung cancer: systemic inflammation and functional impairment without activation of skeletal muscle ubiquitin proteasome system. *Lung Cancer* 2012;**76**:112–7.

43. Baracos VE, DeVivo C, Hoyle DH, Goldberg AL. Activation of the ATP-ubiquitin-proteasome pathway in skeletal muscle of cachectic rats bearing a hepatoma. *Am J Physiol* 1995;**268**:E996–1006.

44. Costelli P, Bossola M, Muscaritoli M, Grieco G, Bonelli G, Bellantone R, *et al*. Anticytokine treatment prevents the increase in the activity of ATP-ubiquitin-and Ca(2+)-dependent proteolytic systems in the muscle of tumour-bearing rats. *Cytokine* 2002;**19**:1–5.

45. Costelli P, Muscaritoli M, Bossola M, Penna F, Reffo P, Bonetto A, *et al*. IGF-1 is downregulated in experimental cancer cachexia. *J Physiol Regul Integr Comp Physiol* 2006;**291**:R674–83.

46. Mastrocola R, Reffo P, Penna F, Tomasinelli CE, Boccuzzi G, Baccino FM, *et al*. Muscle wasting in diabetic and in tumor-bearing rats: role of oxidative stress. *Free Radic Biol Med* 2008;**44**:584–93.

47. Acharyya S, Butchbach ME, Sahenk Z, Wang H, Saji M, Carathers M, *et al*. Dystrophin glycoprotein complex dysfunction: a regulatory link between muscular dystrophy and cancer cachexia. *Cancer Cell* 2005;**8**:421–32.

48. Aulino P, Berardi E, Cardillo VM, Rizzuto E, Perniconi B, Ramina C, *et al*. Molecular, cellular and physiological characterization of the cancer cachexia-inducing C26 colon carcinoma in mouse. *BMC Cancer* 2010;**10**:363.

49. Costelli P, Muscaritoli M, Bonetto A, Penna F, Reffo P, Bossola M, *et al*. Muscle myostatin signalling is enhanced in experimental cancer cachexia. *Eur J Clin Invest* 2008;**38**:531–538.

50. Fang J, Rhyasen G, Bolanos L, Rasch C, Varney M, Wunderlich M, *et al*. Cytotoxic effects of bortezomib in myelodysplastic syndrome/acutemyeloid leukemia depend on autophagy-mediated lysosomal degradation of TRAF6 and repression of PSMA1. *Blood* 2012;**120**:858–67.

51. Li C, Johnson DE. Bortezomib induces autophagy in head and neck squamous cell carcinoma cells via JNK activation. *Cancer Lett* 2012;**314**:102–7.

52. Granato M, Santarelli R, Lotti LV, Di Renzo L, Gonnella R, Garufi A, *et al*. JNK and macroautophagy activation by bortezomib has a pro-survival effect in primary effusion lymphoma cells. *PLoS One* 2013;**8**:e75965.

53. Min H, Xu M, Chen ZR, Zhou JD, Huang M, Zheng K, *et al*. Bortezomib induces protective autophagy through AMP-activated protein kinase activation in cultured pancreatic and colorectal cancer cells. *Cancer Chemother Pharmacol* 2014;**74**:167–76.

54. Periyasamy-Thandavan S, Jackson WH, Samaddar JS, Erickson B, Barrett JR, Raney L, *et al*. Bortezomib blocks the catabolic process of autophagy via a cathepsin-dependent mechanism, affects endoplasmic reticulum stress and induces caspase-dependent cell death in antiestrogen-sensitive and resistant ER+ breast cancer cells. *Autophagy* 2010;**6**:19–35.

55. Kao C, Chao A, Tsai CL, Chuang WC, Huang WP, Chen GC, *et al*. Bortezomib enhances cancer cell death by blocking the autophagic flux through stimulating ERK phosphorylation. *Cell Death Dis* 2014;**5**:e1510.

56. Funderburk SF, Wang QJ, Yue Z. The beclin 1-VPS34 complex: at the crossroads of autophagy and beyond. *Trends Cell Biol* 2010;**20**:355e362.

57. Bonetto A, Penna F, Minero VG, Reffo P, Bonelli G, Baccino FM, *et al*. Deacetylase inhibitors modulate the myostatin/follistatin axis without improving cachexia in tumor-bearing mice. *Curr Cancer Drug Targets* 2009;**9**:608–16.

58. Costelli P, Reffo P, Penna F, Autelli R, Bonelli G, Baccino FM. Ca(2+)-dependent proteolysis in muscle wasting. *Int J Biochem Cell Biol* 2005;**37**:2134–46.

59. Penna F, Costamagna D, Pin F, Camperi A, Fanzani A, Chiarpotto EM, *et al*. Autophagic degradation contributes to muscle wasting in cancer cachexia. *Am J Pathol* 2013;**182**:1367–78.

60. Sandri M. Protein breakdown in muscle wasting: role of autophagy-lysosome and ubiquitine proteasome. *Int J Biochem Cell Biol* 2013;**45**:2121–2129.

61. Wing SS. Deubiquitinases in skeletal muscle atrophy. *Int J Biochem Cell Biol* 2013;**45**:2130–5.

62. Zhang L, Tang H, Kou Y, Li R, Zheng Y, Wang Q, *et al*. MG132-mediated inhibition of the ubiquitin-proteasome pathway ameliorates cancer cachexia. *J Cancer Res Clin Oncol* 2013b;**139**:1105–15.

63. Xing SS, Shen CC, Godard MP, Wang JJ, Yue YY, Yang ST, *et al*. Bortezomib inhibits C2C12 growth by inducing cell cycle arrest and apoptosis. *Biochem Biophys Res Commun* 2014;**445**:375–80.

64. Cavaletti G, Jakubowiak AJ. Peripheral neuropathy during bortezomib treatment of multiple myeloma: a review of recent studies. *Leuk Lymphoma* 2010 Jul;**51**:1178–87.

65. Enrico O, Gabriele B, Nadia C, Sara G, Daniele V, Giulia C, *et al*. Unexpected cardiotoxicity in haematological bortezomib treated patients. *Br J Haematol* 2007;**138**:396–7.

66. Nowis D, Maczewski M, Mackiewicz U, Kujawa M, Ratajska A, Wieckowski MR, *et al*. Cardiotoxicity of the anticancer therapeutic agent bortezomib. *Am J Pathol* 2010;**176**:2658–68.

67. Xiao Y, Yin J, Wei J, Shang Z. Incidence and risk of cardiotoxicity associated with bortezomib in the treatment of cancer: a systematic review and meta-analysis. *PLoS One* 2014;**9**:e87671.